American Journal of Modern Physics
2022; 11(1): 1-6
http://www.sciencepublishinggroup.com/j/ajmp
doi: 10.11648/j.ajmp.20221101.11
ISSN: 2326-8867 (Print); ISSN: 2326-8891 (Online)

Influence of the Magnetic Field on the Diffusion Capacitance of a Serial Vertical Junction Silicon Solar Cell in Frequency Modulation

Mountaga Boiro, Babou Dione, Ibrahima Toure, Adama Ndiaye, Amadou Diao

Department of Physics, Laboratory of Semiconductors and Solar Energy, Faculty of Sciences and Techniques, University of Cheikh Anta Diop, Dakar, Senegal

Email address:
mountagabr@gmail.com (M. Boiro), adiao07@gmail.com (A. Diao)

To cite this article:
Mountaga Boiro, Babou Dione, Ibrahima Toure, Adama Ndiaye, Amadou Diao. Influence of the Magnetic Field on the Diffusion Capacitance of a Serial Vertical Junction Silicon Solar Cell in Frequency Modulation. *American Journal of Modern Physics*. Vol. 11, No. 1, 2022, pp. 1-6. doi: 10.11648/j.ajmp.20221101.11

Received: January 10, 2022; **Accepted**: February 4, 2022; **Published**: February 25, 2022

Abstract: In this work, a theoretical study of the effect of the magnetic field on the minority charge carrier density and the diffusion capacity of a silicon solar cell with vertical junction in series in dynamic frequency regime, is done. From the relative continuity equation of the minority charge carriers' density we establish the boundary condition at the junction and the base medium. The expression of the density of minority carriers of charges in the base, allows us to determine the capacity of diffusion of the solar cell according to the magnetic field, the frequency of modulation, the wavelength of illumination and a junction recombination velocity. The profile of the diffusion coefficient allowed us to make a choice on the values of the magnetic field. These values of the magnetic field intensity will be fixed throughout this article. Each value of the magnetic field strength corresponds to a well-defined value of the resonance frequency. We obtained two ranges of illumination wavelengths from the minority charge carrier' density profile. The influence of the magnetic field on the diffusion coefficient, of the density of minority charge carriers in short-circuit and open-circuit conditions and of the diffusion capacity, for a specific wavelength, is theoretically studied.

Keywords: Vertical Junction Solar Cell, Frequency Modulation, Cut-off Frequency, Magnetic Field, Wavelength, Diffusion Capacity, Junction Recombination Velocity

1. Introduction

Photovoltaic conversion is carried out by a solar cell whose conversion efficiency depends on the nature of the semiconductor structure, its technique and its manufacturing processes [1]. Several studies have been conducted on conventional monofacial or bifacial solar cells in monocrystalline or polycrystalline silicon with a back surface field (BSF) cells [2-4]. The authors showed that the diffusion capacity decreases with the magnetic field and the doping rate in the base. Solar cells may be vertical parallel [5, 6], or vertical series [7, 8], and under different static [9], transient [10] and frequency dynamic regimes [11]. Thus, such a structure makes it possible to decouple the absorption axes of the photons and to collect carriers, which offers more degrees of freedom for optimization compared to conventional horizontal junctions. The current in this device is mainly lateral, the mass losses of resistance in the transmitter area and the electrodes are negligible. As a result, this architecture has a high conversion efficiency under a very high flow concentration [12]. A study of the effect of the applied magnetic field on the diffusion capacity of solar cell with vertical junction series under monochromatic illumination in frequency modulation is proposed.

2. Theory

A series vertical junction silicon solar cell of type n+-p-p+ [13] under an applied magnetic field, is shown in figure 1.

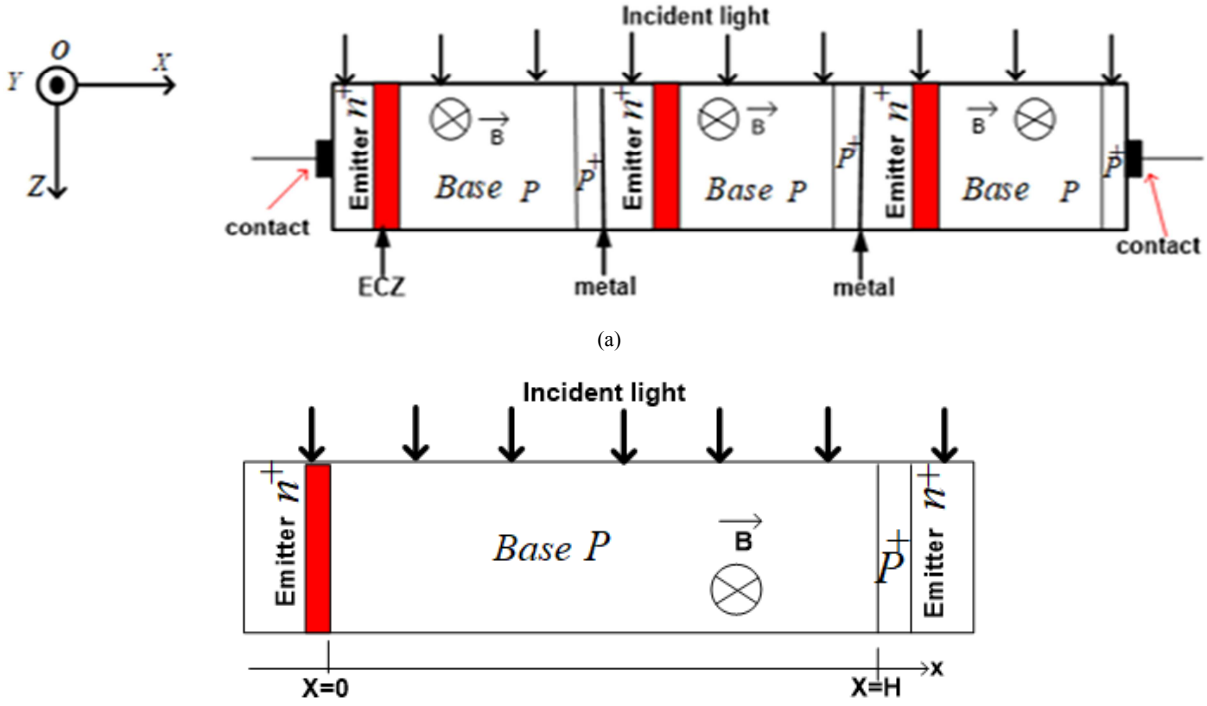

Figure 1. *(a) A series vertical junction solar cell with an applied magnetic field, (b) A single structure of a vertical junction solar cell with an applied magnetic field.*

H is the total thickness of the base. The magnetic field vector B is perpendicular to the (xoz) plane. When the solar cell is illuminated with light, the photogenerated minority carriers' in the base are governed by the continuity equation [14]:

$$D^*.\frac{\partial^2\delta(x,z,t)}{\partial x^2}-\frac{\delta(x,z,t)}{\tau}=-G(z,t)+\frac{\partial\delta(x,z,t)}{\partial t} \quad (1)$$

Where x and z, respectively, are variables along x-axis and z-axis; τ is the mean lifetime of the minority carriers; t is the time, $\delta(x,z,t)$ is the minority carriers' density in the base. D* is the complex diffusion coefficient of the minority carriers in function of the magnetic field and frequency modulation, whose expression is given by [1]:

$$D^*=\frac{D\left[\left(1+\tau^2(\omega_r^2+\omega^2)\right)+i\omega\tau(\tau^2(\omega_r^2-\omega^2)-1)\right]}{\left(1+\tau^2(\omega_r^2-\omega^2)\right)^2+4\tau^2\omega^2} \quad (2)$$

Where D is the diffusion coefficient of the minority carriers without applied magnetic field [15, 16]; ω_r is the cyclotron angular frequency; ω is the incident angular frequency that is related to the frequency modulation f, by: $\omega=2\pi f$.
The generation rate is given by [17]:

$$G(z,t)=g(z).e^{i\omega t} \quad (3)$$

With g(z) the spatial component and $e^{i\omega t}$ the temporal component of the generation rate, ω the angular frequency, t the time and *i* the complex imaginary. The expression of the generation rate g (z) is [18]:

$$g(z)=\phi.\alpha.(1-R)e^{-\alpha.z} \quad (4)$$

Where ϕ is the monochromatic incident fluency of light, α the monochromatic absorption coefficient of the material, and R the monochromatic reflection coefficient of the material.
The density of the minority carriers' is given [19]:

$$\delta(x,z,t)=\delta(x,z).e^{i\omega t} \quad (5)$$

Where δ(x, z) is the spatial part.
By substituting (3) and (5) in (1), we obtain:

$$\frac{\partial^2\delta(x,z)}{\partial x^2}-\frac{\delta(x,z)}{L^{*2}}=-\frac{g(z)}{D^*} \quad (6)$$

Where L^* is the complexe diffusion length that depends on both magnetic field and frequency modulation. Its expression is:

$$L^{*2}=\tau.D^* \quad (7)$$

A general solution of (6) is given as:

$$\delta(x,z)=K_1.e^{\frac{x}{L^*}}+K_2.e^{-\frac{x}{L^*}}+\frac{L^{*2}}{D^*}.\phi.\alpha.(1-R).e^{-\alpha.z} \quad (8)$$

The coefficients K_1 and K_2 can be determined by the following boundaries conditions [11, 20, 21].

1. At the Emitter-base junction (x = 0):

$$D^*.\frac{\partial\delta(x,z)}{\partial x}\Big|_{x=0}=\mathrm{Sf}.\delta(x,z)|_{x=0} \quad (9)$$

2. In the middle of the base (x = H/2):

$$\left.\frac{\partial\delta(x,z)}{\partial x}\right|_{x=\frac{H}{2}} = 0 \qquad (10)$$

Where Sf is the junction recombination velocity [21, 22] which is related to the photogenerated minority carriers' flux across the junction.

3. Results and Discussions

In this part, the profiles of the diffusion coefficient, the minority carriers' density in the base and the diffusion capacitance are presented.

3.1. Diffusion Coefficient

The profile of the diffusion coefficient according to the logarithm of the angular frequency for different values of the magnetic field, is shown in figure 2.

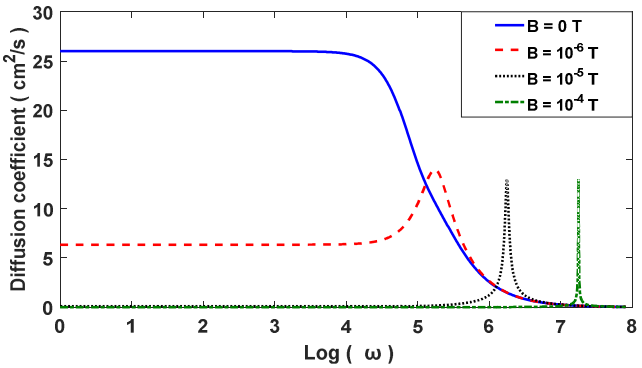

Figure 2. *Diffusion coefficient versus the logarithm of the angular frequency for different values of applied magnetic field.*

In Figure 2, without an applied magnetic field, the curve of the diffusion coefficient versus the logarithm of the angular frequency shows two zones:

1. the first, in the range [0 rad/s; 10^4 rad/s] of low angular frequencies values where the diffusion coefficient is constant. It corresponds to the quasi-static regime where there is no delay between the optical excitation of the minority carriers and their response to diffuse in the base;
2. the second, in the range [10^4 rad/s; 10^8 rad/s] of relative high angular frequencies values where the diffusion coefficient decreases with the increase of the angular frequency. This zone corresponds to the frequency regime, where there is a phase shift between the optical excitation of the minority carriers and their response.

When an applied magnetic field, the curves of the diffusion coefficient versus the logarithm of the angular frequency, show a few peaks of resonance that are obtained when the modulation frequency is equal to the cyclotron frequency (frequency of the electron in its orbit in the presence of the magnetic field) [23, 24]. This modulation frequency that corresponds to a peak of resonance, is called the resonance angular frequency ω_r. For a given curve, there is a zone corresponding to the quasi-static regime, a resonance zone and a decay zone of the diffusion coefficient. We note that the zone of the quasi-static regime is being widened from one curve to another when increasing the applied magnetic field. The upper limit value of the angular frequency of the quasi-static regime, are equal to the cut-off frequency ω_c. The amplitude of the diffusion coefficient diminishes with the increase of the magnetic field and this situation implies a degradation of the solar cell properties.

In the table 1, a few values of resonance frequencies and cut-off frequencies are given for different values of the applied magnetic field.

Table 1. *A few values of the resonance angular frequency ω_r and cut-off frequency ω_c for different magnetic field values.*

Magnetic field B(T)	0	10^{-6}	10^{-5}	10^{-4}
Resonance frequency ω_r (rad/s)	0	$1.75.10^5$	$1.75.10^6$	$1.75.10^7$
Cut-off frequency ω_c (rad/s)	10^4	3.10^4	4.10^5	3.10^6

An increase of the applied magnetic field corresponds also to an increase of the resonance frequency and the cut-off frequency.

3.2. Density of the Minority Carriers

The profile of the minority carriers' density according to the wavelength, for different values of the applied magnetic field, is shown in figure 3.

In Figure 3, the three curves of the minority carriers 'density according to the wavelength have the same behavior. In the range of wavelengths [0.3µm; 0.86µm], the density of the minority carriers increases with the wavelength. The absorption of incident photons in the bulk of the base, increases; this leads to an increased photogenerated of the minority carriers. However, in the interval of wavelength [0.86µm; 1.2µm], the density of the minority carriers decreases with the wavelength. The absorption of incident photons in the bulk of the solar cell, decreases: there is a low photogenerated minority carriers. For a wavelength greater than of the threshold wavelength (λ=1.1 µm), the solar cell becomes transparent and there is any photogenerated minority carriers.

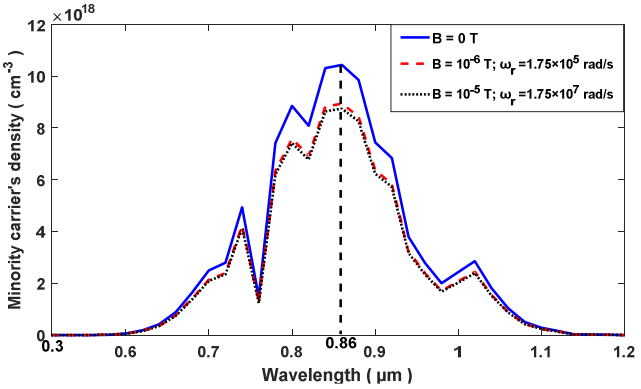

Figure 3. *Density of the minority carriers versus the wavelength for different values of the magnetic field. with z = 0.002 cm.*

Without an applied magnetic field (B = 0T), we note that the amplitude of the minority carriers' density is higher than those corresponding to an applied magnetic field. For all three

curves, the density of the minority carriers is maximum at a specific wavelength $\lambda = 0.86\ \mu m$ where the gradient of the density is equal to zero.

In figure 4, the profile of the minority carriers' density according to the base deph, for different values of the magnetic field, in short-circuit situation, is presented.

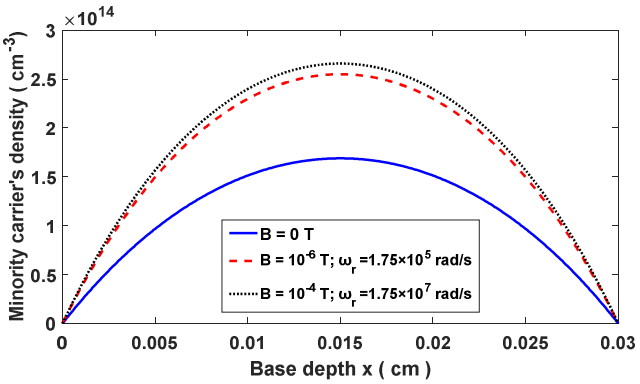

Figure 4. *Density of the minority versus the base depth for different values of the applied magnetic field. z = 0.002 cm; λ = 0.86μm; Sf = 6.10^6cm/s.*

For a given curve, the density of the minority carriers increases with the base depth of the solar cell towards a maximum density that corresponds to the middle of the base thickness at the depth x = 0.015cm. Beyond this depth, the density of the minority carriers decreases. We obtain three zones:

1. the first zone, for $0 \leq x < 0.015cm$ the gradient of the minority carriers' density is positive: this fact corresponds to a passage of the photogenerated minority carriers across the junction. The photogenerated minority carriers in the vicinity of the junction have sufficient kinetic energy to cross it in order to produce a photocurrrent;
2. the second, at the junction x = 0.015 cm, the gradient of the minority carriers' density is zero. There is a storage of the photogenerated minority carriers witch have not enough kinetic energy to cross the junction;
3. the third, for 0.015 cm$< x < 0.03\ cm$, the gradient of the minority carriers' density is positive as the first zone. In this zone, the density of the minority carriers decreases with the increase of the base. The photogenerated minority carriers do not recombine since they have sufficient kinetic energy to cross the junction around the position $x = 0.03$ cm.

The density of the minority carriers increases with the applied magnetic field.

An applied magnetic field slows down the diffusion of photogenerated minority carriers and deflects them form their initial trajectories towards the lateral surfaces of the base, while at the position $x = 0.015$ cm there is a storage of photogenerated minority carriers in the base volume of the solar cell.

In Figure 5, the profile of the minority carriers' density according to the base depth for different values of the magnetic field, in open circuit situation, is presented:

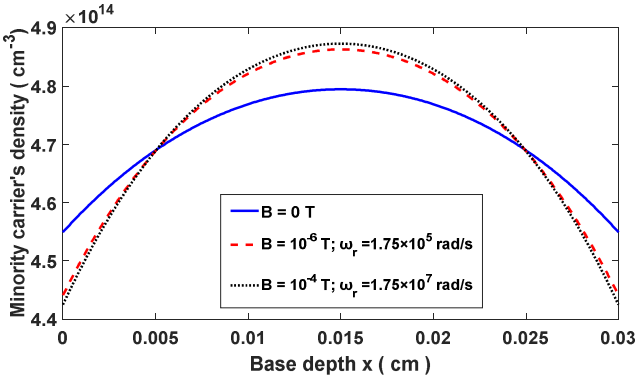

Figure 5. *Density of the minority carriers versus the base thickness for different values of the magnetic field. z=0.002 cm; λ=0.86μm; Sf=2.10^2cm/s.*

In Figure 5, the three curves of the minority carriers' density according to the base depth for different values of the magnetic field, have the same behavior. For a given curve, the minority carriers' density increases with the base depth in the interval [0 cm; 0.015 cm [while in the interval] 0.015 cm; 0.03 cm], the minority carriers' density decreases with the base depth. At the depth that corresponds to x = 0.015cm, the density of the minority carriers is at its maximum: the gradient of the density at this position is zero and the photogenerated minority carriers are blocked.

When a magnetic field is applied, the three curves of the minority carriers' density are intercepted in two particular positions x = 0.005 cm and x = 0.025 cm of the base depth. In the interval [0.005cm; 0.025cm], the amplitude of the minority carriers' density increases in the bulk of the base with the increase of the magnetic field. But in the intervals [0 cm; 0.005 cm] and [0.025 cm; 0.03 cm], the minority carriers' density decreases with the increase of the magnetic field: here the increase of both the magnetic field and the angular frequency resonance leads to a lower photogenerated minority carriers around the junctions; a part of these photogenerated carriers is recombined at the surface densiy of states and the others are blocked in the base.

From the position x = 0 cm to x = 0.005 cm in one hand and x = 0.025 cm to x = 0.03 cm in the other hand, we obtain a base thickness that is equal to 0.005 cm which delimits the space charge region (SCR) from each of the junctions of the solar cell.

3.3. Diffusion Capacitance

The space charge region of a solar cell can be considered as a plan capacitance [25, 26]. This diffusion capacitance of the solar cell can be resulted to the charge carrier's density variation during their diffusion process in the space charge region [27, 28]. The expression of the diffusion capacitance can be given as [22, 29]:

$$C(Sf, \lambda, \omega, B) = \frac{q.n_i^2}{N_b.V_T} + \frac{q}{V_T} \times \delta(x,z)|x = 0 \qquad (11)$$

Where n_i is the intrinsic concentration of the minority carriers; N_b the doping rate in atoms acceptors in the base; V_T the thermal voltage.

The profile of the diffusion capacitance of the solar cell, for

different values of the magnetic field, according to the junction recombination velocity is presented in figure 6:

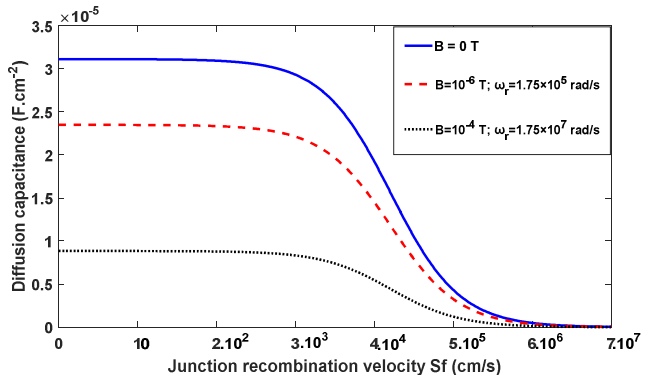

Figure 6. *Diffusion capacitance versus junction recombination velocity for different values of the magnetic field λ= 0.86 µm.*

All the three curves that are presented in figure 6, have the same behavior. For a given curve, the diffusion capacitance is constant slightly for a junction recombination velocity lower than $Sf = 3.10^3\ cm/s$ and its value corresponds to the open-circuit diffusion capacitance C_{co}. For a junction recombination velocity that is upper than $Sf = 3.10^3\ cm/s$, the diffusion capacitance decreases and tends towards to the short circuit diffusion capacitance C_{cc} which can be obtained with $Sf = 6.10^6 cm/s$.

The decrease of the diffusion capacitance from the value of C_{co} to the value of C_{cc}, is due both of the space charge zone extension and the lack of blocked photogenerated carriers that have enough kinetic energy to cross the junction. With an applied magnetic field, the amplitude of the diffusion capacitance decreases and the C_{co} and C_{cc} values decrease too.

4. Conclusion

In our study, the effects of the magnetic field, the angular frequency and the wavelength on minority carriers'density, have been presented. The diffusion capacitance of a serial vertical-junction silicon solar cel, is also depicted. The diffusion capacitance decreases with the increase of the magnetic field and the angular frequency while the minority carriers' density increases in a defined intervals of the base depth. The obtained values of the open-circuit diffusion capacitance, are higher than that of the short circuit diffusion capacitance. We noted that the solar cell electrical and diffusion properties are degraded.

We have considered a non-degenerated density of states; in the future, we will take into account of the degenerated density of states and the contribution of the emitter in this study.

Acknowledgements

We would like to acknowledge the Solar Energy and Semi-conductors Laboratory of the Faculty of Sciences and Techniques of the Cheikh Anta Diop University/Dakar-Senegal for supporting this work.

References

[1] Amadou Diao, N. Thiam, M. Zoungrana, G. Sahin, M Ndiaye, G Sissoko, (2014). Diffusion Coefficient in Silicon Solar Cell with Applied Magnetic Field and under Frequency: Electric Equivalent Circuits. World Journal of Condensed Matter Physics, 4, 84-92.

[2] Equer, B. (1993). Energie solaires photovoltaïque, 1, Collection Ellipses.

[3] Lago-Aurrekoetxea, R. M., Del Can Izo, C., Pou, I., & Luque, A. (2001). Fabrication Process for Thin Silicon Solar Cells. 17th European PVSEC, Munich, 1519-1522.

[4] Schneider, A., Gerhards, C., Huster, F., Neu, W., Spiegel, M., Fath, P., Bucher, E., Young, R. J. S., Prince, A. G., Raby, J. A., & Carollal, A. F. (2001). BSF for Thin Screen-Printed Multicrystalline Si Solar Cells. 17th European PVSEC, Munich, 1768-1771.

[5] Bordin, N., Kreinin, L., & Eisenberg, N. (2001). Determination of recombination parameters of bifacial silicon cells with a two layer step-liked effect distribution in the base region. Proc. 17th European PVSEC, 1495-1498.

[6] P. Ooshaksaraei, K. Sopian, R. Zulkifli, M. A. Alghoul, and Saleem H. Zaidi. (2013). Characterization of a Bifacial Photovoltaic Panel Integrated with External Diffuse and Semimirror Type Reflector. International Journal of Photoenergy, 1-7. doi.org/10.1155/2013/465837.

[7] Stephen Kaye, Pasadena, and Louis Garasi. (1967). Solar cell configuration. United States Patent, 3.

[8] G. C. Jain, S. N. Singh and R. K. Kotnala. (1983). Diffusion length determination in n+-p-p+ structure based silicon solar cells from the intensity dependence of the short-circuit current for illumination from the p+ sid. Solar Cells. 8. 239-248.

[9] M. I. Ngom, M. S. Diouf, A. Thiam, Ould El Moujtaba, Mohamed Abderrahim and G. Sissoko. (2015). Influence of Magnetic Field on the Capacitance of a Vertical Junction Parallel Solar Cell in Static Regime, Under Multispectral Illuminatio. International Journal of Pure & Applied Sciences & Technology. 31 (2). 65-75.

[10] K. S. Rabbani and D. S. Lamb. (1981). A quick method for the determination of bulk generation lifetime in semiconductors from pulsed MOS capacitance measurements. Solid-State Electronics. 24. 661-664.

[11] Thiam, Nd., Diao, A., Ndiaye, M., Dieng, A., Thiam, A., Sarr, M., Maiga, A. S. and Sissoko, G. (2012). Electric Equivalent Models of Intrinsic Recombination Velocities of a Bifacial Silicon Solar Cell under Frequency Modulation and Magnetic Field Effect. Research Journal of Applied Sciences, Engineering and Technology. 4. 4646-4655.

[12] Sater BL, Sater ND. (2003). High voltage silicon VMJ solar cells for up to 1000 suns intensities. In Conference Record of the 29th IEEE Photovoltaic Specialists Conference, New Orleans. 1019–1022.

[13] Pozner, R., Segev, G., Sarfaty, R., Kribus, A., Rosenwaks, Y. (2011). Vertical junction Si cells for concentrating photovoltaics. Progress in Photovoltaics Research and Applications. 20 (2). 197–208. doi: 10.1002/pip.1118.

[14] W. V. Roosbroeck. (1953). The transport of added current carriers in a homogeneous semiconductor. Physical. Revue 91.

[15] Seeger, K. (1973). Semiconductor Physics. 1st edition. doi.org/10.1007/978-3-7091-4111-3.

[16] Sze, S. M. (1981). Physics of Semiconductor Devices. John Wiley & Sons.

[17] J. N., and G. Hasnain. (1995). Frequency dependent hole diffusion in InGaAs double heterostructures. Appl. Phys. Lett. 67 (15). 2203 – 2205.

[18] José Furlan and Slavko Amon. (1985). Approximation of the carrier generation rate in illuminated silicon. Solid State Electronics. 28 (12). 1241 – 1243.

[19] Th. Flohr and R. Helbig. (1989). Determination of minority-carrier lifetime and surface recombination velocity by Optical-Beam-Induced-Current measurements at different light wavelengths.. J. Appl. Phys. 66 (7). 3060 – 3065.

[20] Madougou, S., Made, F., Boukary, M. S., & Sissoko. (2007). Recombination parameters determination by using Internal Quantum Efficiency (IQE) data of bifacial silicon solar cells. Advanced Materials Research. 18-19. 313-324.

[21] G. Sissoko, S. Sivoththanam, M. Rodot, P. Mialhe "Constant illumination-induced open circuit voltage decay (CIOCVD) method, as applied to high efficiency Si Solar cells for bulk and back surface characterization" 11th European Photovoltaic Solar Energy Conference and Exhibition, poster 1B, 12-16 October, 1992, pp. 352-54, Montreux, Switzerland.

[22] H L Diallo, A. Wereme, A S Maïga et G. Sissoko. (2008). Nouvelle approche des vitesses de recombinaison de jonction et de surface arrière dans une étude de modélisation 3D d'une cellule solaire en silicium polycristallin. Eur. Phys. J. Appl. Phys. 42. 203–211.

[23] C. Kittel. (1972). Introduction à la Physique de l'Etat Solide. 284-285.

[24] M. Cardona. (1969). Modulation Spectroscopy. Solid State Physics.

[25] A. Thiam, M. Zoungrana, H. Ly Diallo, A. Diao, N. Thiam, S. Gueye, M. M. Deme, M. Sarr and G. Sissoko. (2013). Influence of Incident Illumination Angle on Capacitance of a Silicon Solar Cell under Frequency Modulation. Research Journal of Applied Sciences, Engineering and Technology. 4. 1123-1128.

[26] S. Mbodji, M. Mbow, F. I. Barro and G. Sissoko. (2010). A 3d model for thickness and diffusion capacitance of emitter-base junction in a bifacial polycrystalline solar cell. Global journal of pure and applied sciences. 16 (4). 469- 477.

[27] A. Jakubowski. (1981). Graphic method of substrate doping determination from C-V characteristics of MIS capacitors. Solid-state electronics. 24 (10). 985-987.

[28] G. Sahin, M. Dieng, M. A. Ould El Moujtaba, M. I. Ngom, A. Thiam and G. Sissoko. (2015). Capacitance of Vertical Parallel Junction Silicon Solar Cell under Monochromatic Modulated Illuminatio. Journal of Applied Mathematics and Physics. 3. 1536-1543.

[29] F. I. Barro, M. Ndiaye, M. Deme, S. Mbodji, E. Ba and G. Sissoko. (2008). Influence of grains size and grains boundaries recombination on the space-charge layer thickness z of emitter-base junction's n+-p-p+ solar cell. Proceedings of the 23rd European Photovaltaic Solar Energy Conference and exhibition. 608-611.